Organic Electronics 13 (2012) 104–113

Contents lists available at SciVerse ScienceDirect

Organic Electronics

journal homepage: www.elsevier.com/locate/orgel

Photocrosslinkable liquid-crystalline polythiophenes with oriented nanostructure and stabilization for photovoltaics

Xuee Li [a], Lie Chen [a,*], Yiwang Chen [a,b,*], Fan Li [a], Kai Yao [b]

[a] Institute of Polymers, Nanchang University, 999 Xuefu Avenue, Nanchang 330031, China
[b] Institute of Advanced Study, Nanchang University, 999 Xuefu Avenue, Nanchang 330031, China

ARTICLE INFO

Article history:
Received 10 September 2011
Received in revised form 9 October 2011
Accepted 18 October 2011
Available online 3 November 2011

Keywords:
Photovoltaics
Conjugated polymers
Fullerene
Liquid crystals

ABSTRACT

A novel stable and photocrosslinkable electron-donor material, liquid-crystalline polythiophene containing cyano-biphenyl mesogenic pendant, namely, poly{3-[6-(4′-cyano-biphenyloxy)hexyl]thiopheneylenethiophene-*alt*-3-(6-bromohexyl)thiophene} (PTcbpTT), was designed and synthesized. The structural anisotropy originating from cyano-biphenyl mesogens can induce the PTcbpTT to assemble into a well ordered morphology and consequently lead to the red-shift absorption, enhanced photoluminescence. The thermal treatment drives further development of the morphology of the copolymer and its blend films mixed with [6,6]-phenyl-C_{61}-butyric acid methyl ester (PCBM), towards a state of microphase separation in the nanometer scale. Furthermore, the bulk heterojunction devices based on the PTcbpTT:PCBM (1:1 wt.%) active layer have been constructed. Without extensive optimization, the LC annealing device yields an enhancement of power conversion efficiency from 0.5% to 1.2%, showing a significantly increased J_{sc} and FF with respect to its untreated counterpart, thanks to the ordered microphase separation channels for charge transportation. The high V_{oc} value of 0.731 V is due to the low HOMO level of PTcbpTT. Unlike devices prepared from PTcbpTT:PCBM blend without UV treatment, photocrosslinked PTcbpTT:PCBM devices are stable even when annealed for two days at the elevated temperature of 150 °C, implying that the photocrosslinked structure dramatically suppresses largescale phase segregation.

1. Introduction

Polymer photovoltaic (PV) cells have attracted considerable attention due to the potential large-area manufacture capability, improved compatibility with low-cost flexible substrates, and the high degree of control over the optoelectronic properties of the conjugated polymers [1–4]. The bulk-heterojunction (BHJ) structure, which has a nanoscale interpenetrating network morphology and is created by blending a p-conjugated polymer as an electron donor and a fullerene derivative as an electron acceptor, has been viewed as a promising device structure for exciton dissociation [5,6]. Although a number of polymer–fullerene combinations have been tested [7,8], BHJ solar cells based on poly(3-hexylthiophene) (P3HT) and the fullerene derivative [6,6]-phenyl-C61-butyric acid methyl ester (PCBM) exhibited quite promising power conversion efficiency (PCE) [9–11].

However, the power conversion efficiency (PCE) is still limited by the space charge effects inherent in the BHJ structure and the unfavorable morphology. Obtaining an ordering bicontinuity of the microphase, which ensures optimum charge-carrier photogeneration, extraction and the transfer to the electrodes, is one of the most critical challenges in organic photovoltaics [12–14]. Various independent approaches, including thermal annealing,

* Corresponding authors. at: Institute of Polymers, Nanchang University, 999 Xuefu Avenue, Nanchang 330031, China. Tel.: +86 791 83969562; fax: +86 791 83969561 (Y. Chen).
E-mail addresses: chenlienc@163.com (L. Chen), ywchen@ncu.edu.cn (Y. Chen).

1566-1199/$ - see front matter © 2011 Elsevier B.V. All rights reserved.
doi:10.1016/j.orgel.2011.10.012

post-fabrication annealing at high temperature, additives, and solvent annealing have been demonstrated to develop a morphology with an optimum phase segregation with crystalline domains of different compositions, leading to the PCE improvement of the blends [15]. But the microstructure of molecular solids, especially when solution processed, depends upon the self-organizing tendencies of the components and hence on both molecular structure and processing route, and is not easy to control [16]. Furthermore, most BHJ polymer solar cells are not thermally stable as subsequent exposure to heat and the microphase separation may alter by large aggregation over time, particularly under device operating conditions [2,17]. Any heat generated by solar emission can be detrimental to the performance of the devices a result of the relatively low glass transition temperature (T_g) of the polymer blend and the miscibility of donor and acceptor materials in the photoactive layer [18]. Several useful methods have been reported to improve the thermal stability of conjugated polymer–fullerene BHJ photovoltaic devices. One approach explored the use of thermally crosslinkable units as a means to prevent phase segregation on one of the materials. However, thermal treatments used to induce crosslinking may be detrimental in that they prevent the annealing processes from being properly carried out [19,20].

Liquid crystal (LC) polymers have been applied as an engineering plastic providing good processability, strength, and elasticity [21,22]. It is generally known that the introduction of LC side group into the main chain allows polymers to form an LC phase as a side-chain LC polymer [23,24], conjugated polymers with an LC phase under appropriate conditions are of particular interest, offering both electrical conductivity and self-organized properties [25–27]. In view of this incorporating a liquid-crystalline (LC) group as a side chain onto the polymer probably can optimize processability, crystalline nanostructure, and control nanoscale morphology of active layer eventually. In our previous studies, we have synthesized liquid-crystalline polyfluorene derivates containing cyanobiphenyl mesogens with alkyl terminal group and found that the spontaneous assembly of the liquid-crystalline molecules pushes PCBM clusters to form an oriented nanodispersing structure [28].

In order to develop a well-ordering morphology with high thermal stability for polymer solar cells (PSCs), herein, we have constructed a novel photocrosslinkable material with cyanobiphenyl mesogens, bromine-functionalized poly{3-[6-(4′-cyano-biphenyloxy)hexyl]thiopheneylenethiophene-*alt*-3-(6-bromohexyl)thiophene} (PTcbpTT), and employed into BHJ photovoltaic devices, to stabilize the BHJ film morphology with minimal disturbance in the packing of the whole systems under heating. The photocrosslinking reaction instead of thermally crosslinking is carried out in the system after a thermal annealing process to provide a stable and ordered microphase separation. The synthetic route to PTcbpTT is depicted in Scheme 1, and the synthesis of high molecular weight, readily soluble copolymers is accomplished by Pd-catalyzed Stille coupling reactions.

2. Results and discussion

2.1. Structural characterization

The synthetic route to the monomer MTcbp and its counterpart copolymer PTcbpTT is outlined in Scheme 1. The structure of PTcbpTT was confirmed by FT-IR, ^{1}H NMR and ^{13}C NMR. The presence of the *cyano* functionality is confirmed by the appearance of FT-IR bands at 2220 cm^{-1} (see Supporting Information, Fig. S1). In Figs. S2 and S3 (top), two signals (7.60 and 4.01 ppm) in the ^{1}H NMR

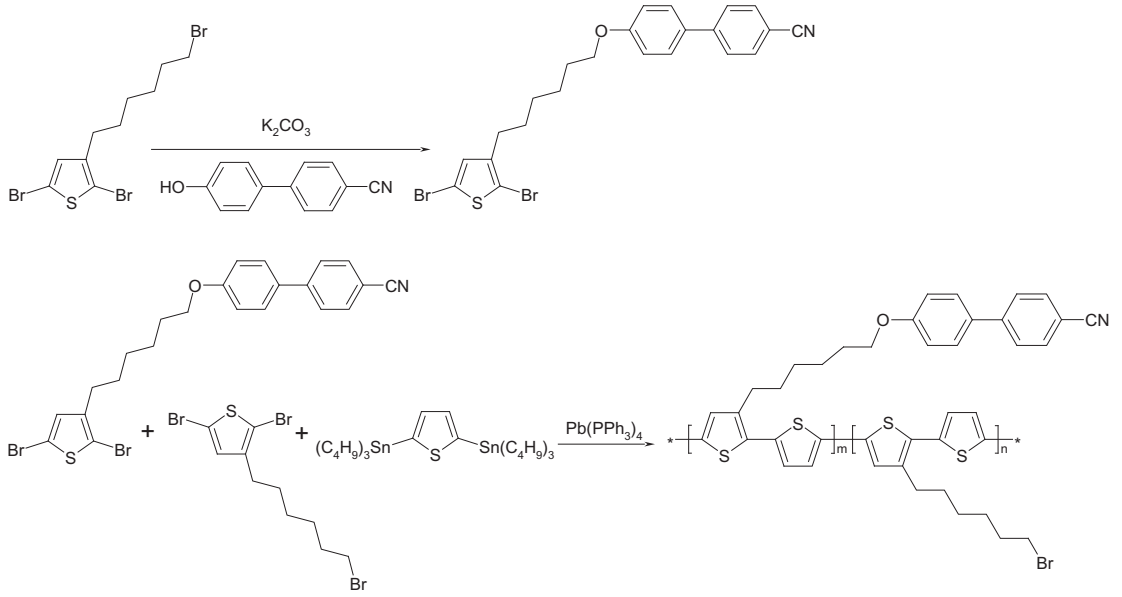

Scheme 1. Synthetic routes for monomer MTcbp and copolymer PTcbpTT.

spectra of MbpT and PTcbpTT are evident from the protons on the cyanobiphenyl rings and methylene for oxygen (CH_2–O), respectively. The ^{13}C NMR spectrum (Fig. S3 (bottom)) of the copolymer also agrees with the molecular structure, and all other resonance peaks can be readily assigned with no unexpected signals found (see Supporting Information for details).

2.2. Thermal stability and liquid crystallinity

The thermal stability of the copolymer is evaluated by TGA under a nitrogen atmosphere. The copolymer exhibits thermally stability with little decomposition at high temperature (about 300 °C), which is ascribed to the mesogenic appendages well wrapping the conjugated backbone to protect them from the perturbations by heat and attacks by the degradative species [29] (Fig. S4). The mesomorphic behavior of PTcbpTT also has been studied by polarizing optical microscopy (POM) (Fig. 1) and differential scanning calorimetry (DSC) (Fig. S5). Both the monomer and copolymer exhibit enantiotopic liquid-crystalline optical anisotropy with a nature of SmA phase when heated or cooled due to the existence of cyanobiphenyl mesogen. However, the less bright and colorful picture of copolymer possibly implies the poor molecular packing in the system. This is because the rigid backbones interfere in the assembly of the mesogens in some extent. The DSC thermogram of MTcbp only shows a mesogens to isotropic transition at 79.1 °C in the second heating cycle, while its k-SmA transition can be observed at 47.3 °C by POM. Also, the DSC thermogram of PTcbpTT exhibits a g-SmA transition at 136.7 °C in the second heating cycle and with the aid of POM, the range of liquid crystallinity of PTcbpTT covers from 136.7 to 179.6 °C. The liquid crystalline property of molecules can be further supported by XRD analysis (Fig. S6). The samples were heated once to produce the anisotropic phase, then frozen by the rapid quenching with liquid nitrogen in order to maintain molecular arrangements in liquid-crystalline phases. The XRD diffractogram of both monomer and copolymer show a sharp reflection at the low angle ($2\theta = \sim 3°$) and a broad peak at the high angle ($2\theta = \sim 20°$), from which a nature of SmA can be derived [29].

2.3. Optical properties

Fig. 2 shows the UV–vis absorption of the pristine films and blend films with PCBM. Also included are the corresponding films after thermal annealing from different temperatures, e.g. 120, 160, 200 °C, associated to the below, at and beyond mesogens states temperature. From Fig. 2A, we can see that as-cast PTcbpTT film possesses the maximum absorption band at around 506 nm, while the absorption bands of all the annealed samples red shift to the long wavelength, and the LC annealed one with crystalline domains shows the maximum red shift about 10 nm. The extra shift is attributed to a improved coplanar of molecules and a well-ordered π–π stacking induced by the orientation of the cyanobiphenyl mesogens after thermal treatment at LC states [30]. And the same situation happens in the case of blend system (Fig. 2B). From the spectra, we can conclude that all of the LC annealed films show the best absorptions than their counterpart species.

The photoluminescence (PL) spectra of the thin films of copolymer PTcbpTT and with PCBM blend produced by excitation with the 430 nm are presented in Fig. 3. The polymers, whether annealed or not, show excellent PL emission, owning to the radiative deactivation of the exciton without dissociation or non-radiative deactivation. The luminescences from the blend samples with the copolymer and PCBM in the films state are almost quenched completely. Relating to the PL intensity of the corresponding pure polymer films, the PL quenching efficiencies in blend films are beyond 92%, and that of the LC state treated film reaches the highest value of 95%. This PL quenching behavior can be explained by intermolecular electron transfer from the photoexcited copolymers to the PCBM. Compare with the other blends (the blend films as-cast, annealing below and beyond the LC state), the LC annealed copolymers tend to form a better pathway for electrons and holes for transporting.

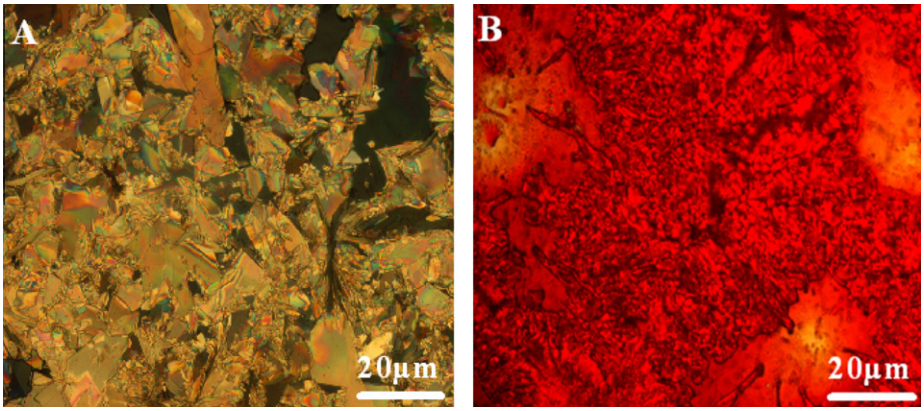

Fig. 1. The mesomorphic textures observed by POM at (A) 55 °C for MTcbp and (B) 160 °C for PTcbpTT under cooling from melt state (cooling rate: 1 °C/min).

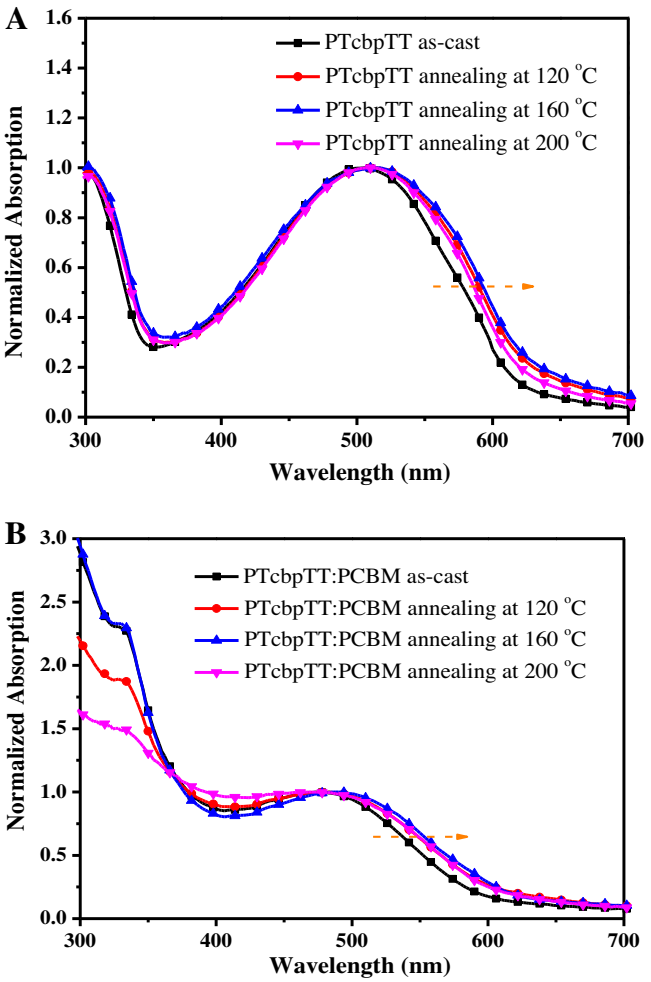

Fig. 2. Optical absorption of thin films of (A) PTcbpTT and (B) PTcbpTT:PCBM under different temperature annealing on a quartz plate.

2.4. Electrochemical study

The electrochemical property is one of the most important properties of the conjugated polymers, and many applications of the conjugated polymers depend on the electrochemical properties. We studied the redox potentials of the polymer by cyclic voltammetry (CV). Fig. S7 shows the cyclic voltammogram of the copolymer film on the Pt electrode. The HOMO energy level of PTcbpTT is calculated to be −5.28 eV based on the onset potential for oxidation at around 0.88 eV. The LUMO energy level is approximately estimated by subtracting the band gap value from the corresponding HOMO level. The optical band-gap (E_g^{opt}) deduced from the absorption edge of thin film spectra is 1.93 eV. So, we can know that the LUMO energy level is −3.35 eV. LUMO offsets of the acceptor and donor must be sufficiently large enough to guarantee energetically efficient charge transfer and, therefore, devices exhibiting higher current output. Fig. 4 reveals that the LUMO energy level of our copolymer is 0.95 eV higher than the LUMO energy level of PCBM, which is well above the required energy for efficient charge separation. It is worthy to note that, in comparison with P3HT, known as the most promising donor, the extra benefit of the copolymer observed from much lower HOMO level would render a higher value of V_{oc} in the fabricated device and enhance the device stability as well.

2.5. Film morphology

The mixing morphology of the polymer and PCBM composite film has proven to be extremely important in determining the photovoltaic properties of PSCs, which mainly affects the interpenetrated network of the donor and the acceptor [31]. The morphology of the active layer was verified by transmission electron microscopy (TEM). Fig. 5 shows morphology of the films of copolymer blended with PCBM as described. Relatively dark regions in the TEM image indicate PCBM-rich regions or aggregates [32]. For the blend before annealing, the interpenetrating networks are not well developed. Both the copolymers and the PCBM aggregate and form serious largescale phase separation (Fig. 5A). After thermal annealing at LC state (160 °C) for 1 h, a fully mixed morphology was formed, and the

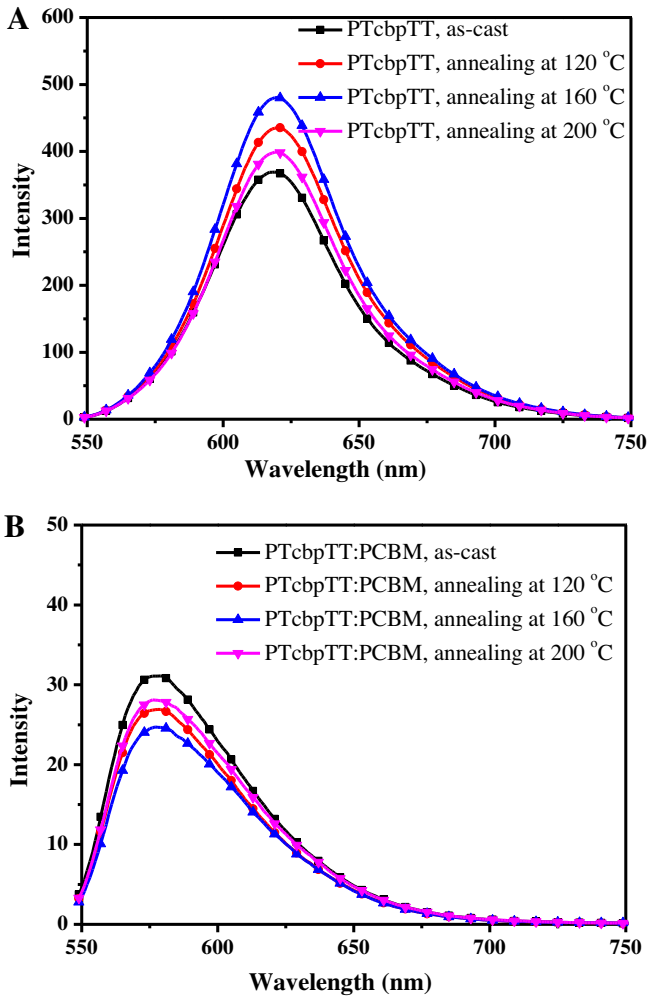

Fig. 3. Photoluminescent spectra for (A) the copolymer films and (B) blend films of copolymer:PCBM (1:1 wt.%) under different temperature annealing on a quartz plate (λ_{ex} = 430 nm).

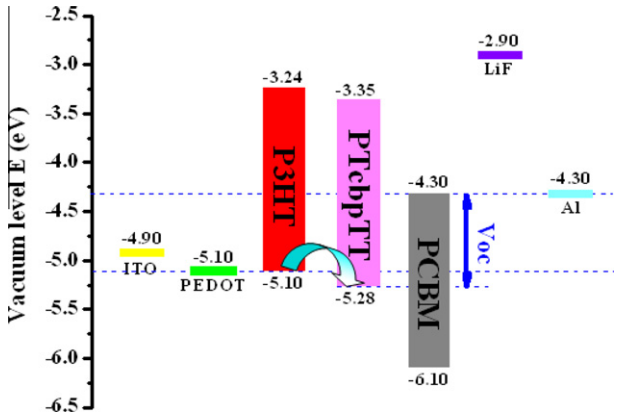

Fig. 4. Energy-level diagram showing the HOMO and LUMO energy levels of PTcbpTT, P3HT, and PCBM.

morphology of the interpenetrating donor–acceptor networks becomes clearer and easily visible, which arises from the self-organization of the PTcbpTT chains oriented in the liquid-crystalline phase. This microscale morphology leads

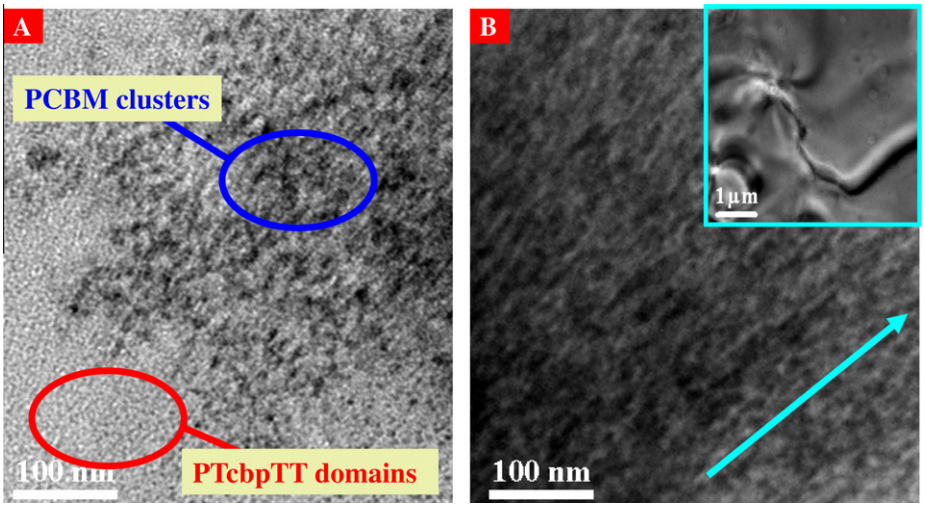

Fig. 5. TEM images of the PTcbpTT:PCBM (1:1 wt.%) blend films spin-cast from DCB (A) before and (B) after annealing at their liquid-crystalline state (the inset shows the macroscale domains).

to the formation of highly ordered domains on the macroscale (Figs. 5B and S8).

The instability of the active layer hinders the application of organic solar cells greatly. Many efforts, such as developing thermo-cleavable polymers [33], elevating the T_g temperature of donor materials [34–36] and forming the crosslinked structures via photocross-linking [18,37] or thermal cross-linking [19,20], have been demonstrated to improve the stability of the active layer. Among those methods mentioned above, photocrosslinking does not interfere with the morphology and the thermal annealing that is often needed during device optimization. Thus, the photocrosslinking method was conducted in our active layer and its impact on morphology of the films was further investigated by the insolubility of the film in organic solvents as monitored by UV–vis absorption spectra. Namely, thin films of the pristine copolymer and the copolymer:PCBM mixture were prepared by spin-coating on quartz substrates, then exposured under UV (λ = 254 nm, 1.9 mW/cm^2) for 0 or 30 min. And pre-annealed (from mesogen state) blend films with or without UV treatment are also present for comparison. The irradiated copolymer films were immersed into DCB for 5 min, followed by rinsing with acetone for a few minutes and then dried under a stream of nitrogen. The UV–vis spectra were measured again in order to check the amount of copolymers remaining on the substrates. Fig. 6A shows the UV–vis spectra of the pristine polymer films before and after the solvent immersion. The film without exposured under UV radiation has only a slight absorption after the solvent immersion, suggesting that PTcbpTT was almost completely dissolved in DCB. On the other hand, the PTcbpTT undergoing UV radiation still remained a strong absorption with about a half of intensity respect to untreated film, indicative of a photocrosslinked structure emerging in the copolymer. We thus speculate that the PTcbpTT copolymers are crosslinked via a radical mechanism initiated by the photochemical cleavage of the C–Br bonds under deep-UV irradiation at 254 nm [38–40]. Similar insolubility of PTcbpTT was also observed in the polymer:PCBM mixture film with and without annealing (Fig. 6B). The absorption of both PTcbpTT and PCBM disappeared completely in the PTcbpTT:PCBM film which without exposured under UV after the immersion into DCB. In contrast, the polymer PTcbpTT in blend films exposured under UV remained its strong light absorption property at ~500 nm after the immersion, while PCBM also present a moderate absorption at 330 nm, as shown in Fig. 6C. This suggests that the result cross-linking net work formed in the blend films not only enhanced the polymer stability, but also prevent the extraction of PCBM from the film to some extent. Furthermore, the absorption bands shapes of the cross-linked and uncross-linked blends with pre-annealing are very similar and no significant shifts in the peak maximum are observed. This is suggestive of little morphology disturbance and the high ordered nanostructure driven by the crystallization of the mesogen-containing polymer and PCBM molecule net work.

2.6. PSC device performances

The current–voltage characteristics under illumination for PV devices with various organic solvents treatment are shown in Fig. 7A. The parameters for these PV cells are summarized in Table 1. It can be seen that the J_{sc} of the PV cell with DCB vapor treatment is larger than those of chloroform (CF) and chlorobenzene (CB)-treated devices. The improvement is attributed to the more efficient self-organization of PTcbpTT. The PCE of the PV cells with CF, CB and DCB treatment are 0.2%, 0.3% and 0.5%, respectively. Although the DCB treatment can effectively induce PTcbpTT chains self-organizing into the more ordered structure, the performance of the PV cells is still poor. Post-thermal annealing from LC states (160 °C) of the PV cells is carried out to further improve the device performance. After liquid-crystalline temperature annealing,

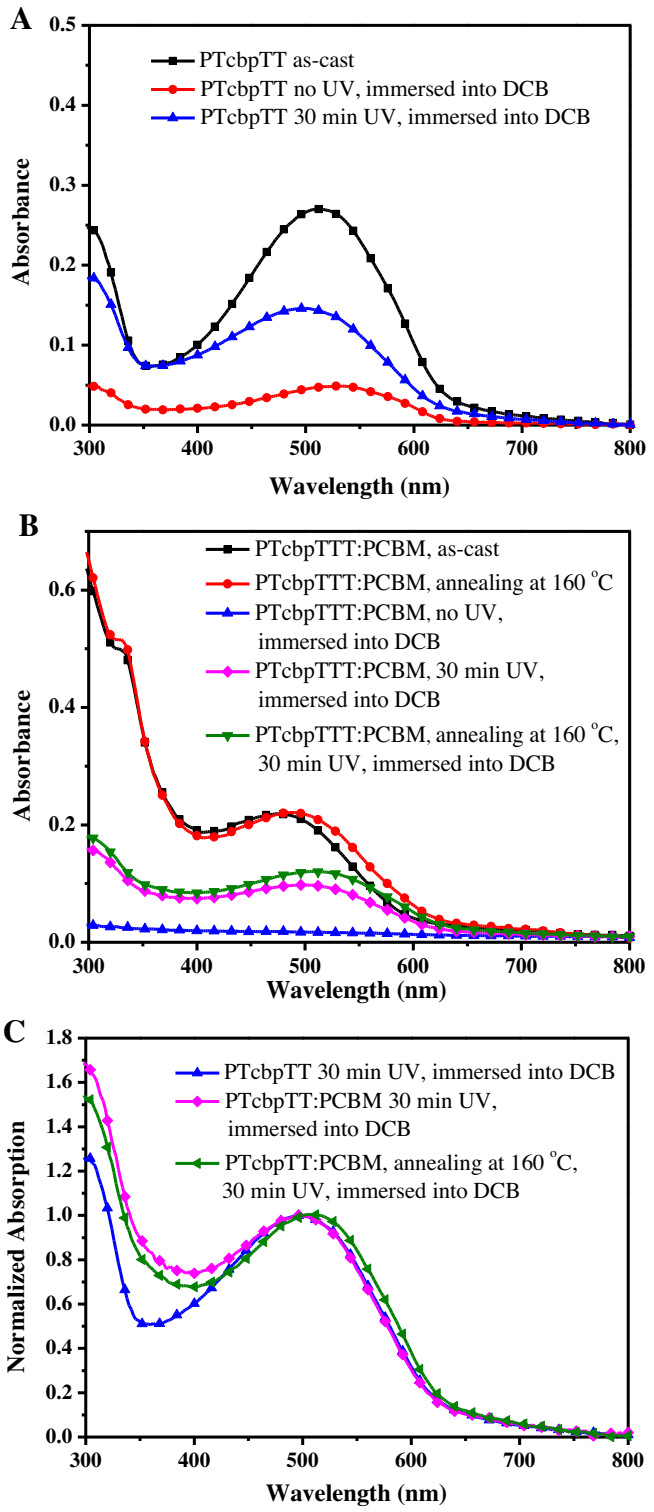

Fig. 6. UV–vis absorption spectra of (A) PTcbpTT, (B) PTcbpTT:PCBM (1:1 wt.%) and (C) all of the photocrosslinked films before and after the immersion into DCB.

the V_{oc} of the DCB-treated solar cell is very similar to that of devices before annealing, whereas its J_{sc} and the *FF* significantly increased from 2.30 and 0.272 to 3.74 and 0.436 upon annealing, respectively. As a result, the PCE

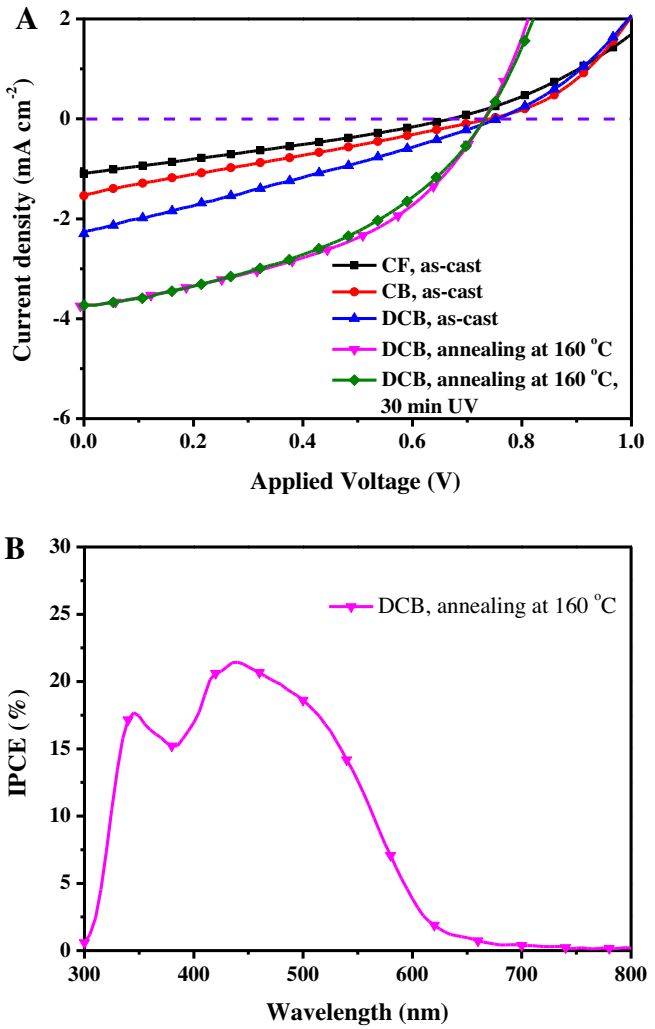

Fig. 7. (A) *J–V* curves of the copolymer photovoltaic cells based on PTcbpTT:PCBM (1:1 wt.%) as-prepared from different solvents and after annealing at their liquid-crystalline state under the illumination of AM 1.5, 100 mW/cm^2. (B) Incident photon-to-current efficiency (IPCE) of photovoltaic cell calculated from the photocurrent under short-circuit condition based on PTcbpTT:PCBM (1:1 wt.%) cast from DCB and annealing at their liquid-crystalline state.

Table 1
Photovoltaic properties of bulk heterojunction solar cells based on PTcbpTT:PCBM (1:1 wt.%) before and after annealing at their liquid-crystalline state.

Compositions of active layer	V_{oc} (V)	J_{sc} (mA/cm^2)	FF	PCE (%)
As-cast (CF)	0.665	1.10	0.283	0.2
As-cast (CB)	0.733	1.54	0.259	0.3
As-cast (DCB)	0.748	2.30	0.272	0.5
As-cast (DCB), 160 °C annealed	0.731	3.74	0.436	1.2
As-cast (DCB), 160 °C annealed, 30 min UV	0.732	3.73	0.418	1.1

increased from 0.5% to 1.2%. Post-thermal annealing of the solvent vapor-treated devices favors activating PCBM molecules to diffuse and aggregate for better electron transport, and LC annealing can simultaneously enhance the packing arrangement of PTcbpTT induced by cyanobiphenyl mesogens and reduce the density of defects at the interface to facilitate the hole transport [41,42]. Interestingly, after further photocrosslinking performed on the LC-annealing device, all of the performance parameters remain no obvious change in respect with the LC-annealing devices, implying the morphology of the active layer did not be disturbance by crosslinking net work, which is consistent with the UV absorption mentioned above and polarizing optical micrographic analysis (discuss later). The incident photon-to-current efficiency (IPCE) spectra of the DCB-treated solar cell annealing at LC state shows two maxima peaks with values of ~18% and ~22% at a wavelength of 345 and 440 nm, respectively (Fig. 7B).

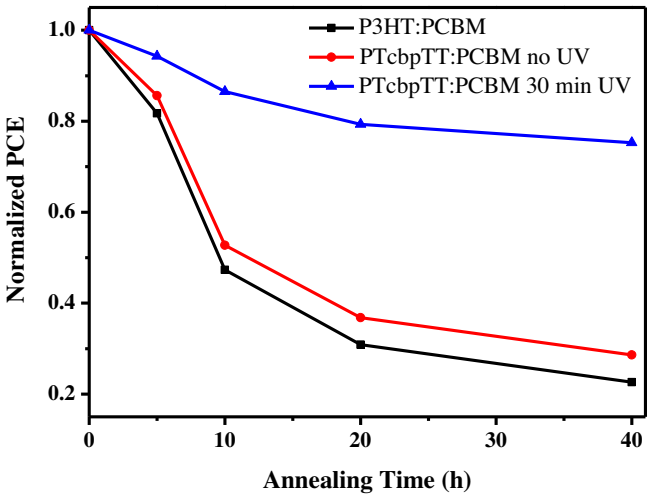

Fig. 8. Efficiencies of P3HT:PCBM and PTcbpTT:PCBM devices annealed at 150 °C for different times. The PTcbpTT:PCBM blends experience with or without exposure to UV. The different devices are prepared under identical condition.

Fig. 8 shows the thermal stability of a PTcbpTT:PCBM BHJ device compared to that of P3HT:PCBM. Two different samples of PTcbpTT:PCBM were prepared from DCB. One film was used without exposure to UV light while another one was exposed to UV light for 30 min, prior to Al deposition. A P3HT:PCBM blended device was also prepared; which was not exposed to UV light and served as a control sample. The device performance of the pristine-P3HT:PCBM blend decreased rapidly to a third of its initial efficiency value after 40 h at 150 °C. Similarly, a control sample of PTcbpTT:PCBM without any UV treatment also showed a rapid decrease in device performance at 150 °C as observed for the P3HT:PCBM blend device. In contrast, the performance of the PTcbpTT:PCBM device treated by UV irradiation exhibits a very stable device performance (~75% initial device efficiency) even after 40 h (~two days)

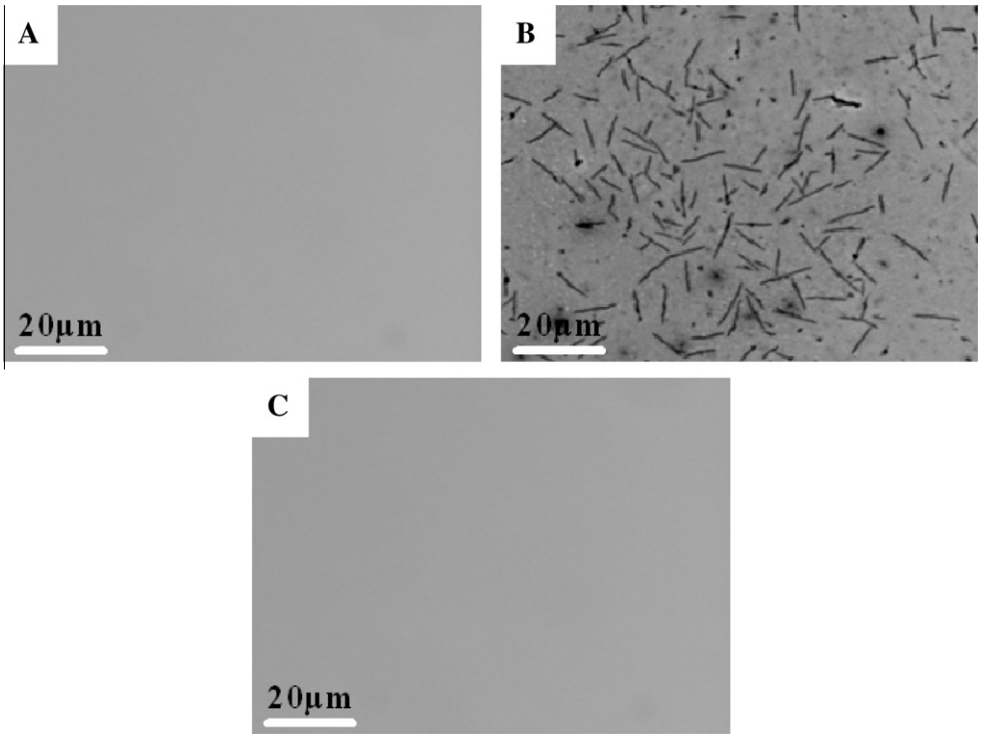

Fig. 9. Optical microscopy images of PTcbpTT:PCBM (1:1 wt.%) blends (A) as cast with no thermal annealing, (B) after 24 h annealing at 150 °C without exposure to UV and (C) after 24 h annealing at 150 °C following exposure to UV for 30 min.

of annealing at 150 °C. This result clearly shows that the photocrosslinking concept holds promise for thermally stable high performance devices.

Polarizing optical micrographic images of PTcbpTT:PCBM (1:1 wt.%) under a variety of conditions described the function of photocrosslinking nanostructure on the device stability. The images shown in Fig. 9A and B demonstrate that thermal annealing at 150 °C induces a big aggregated domain of many needle-like PCBM crystals in the blend film from the untreated film, which response for the sharp decreased performance when annealed at high temperature. In contrast, in Fig. 9C the optical micrograph of the PTcbpTT:PCBM blend crosslinked by UV treatment shows an homogeneous film free of dark PCBM crystals, even heated to 150 °C. These optical micrographs confirm that the photocrosslinking of PTcbpTT copolymers dramatically suppresses large phase segregation and maintains the well-ordered nanoscale morphology.

3. Conclusions

In this work, we have intramolecularly incorporated the mesogenic cyanobiphenyl to photocrosslinkable polythiophenes for the purpose of highly stable and ordered liquid-crystalline conjugated materials, PTcbpTT. The spontaneous orientation of cyanobiphenyl mesogen endows the copolymer and copolymer:PCBM blend films with a well ordered morphology and enhanced properties. The thermal treatment, especially from the liquid-crystalline state, favors the more ordered nanoscale morphology. After radiation by UV, the blend film formed a cross-linking net work which cannot only enhance the polymer stability, but also maintain the ordering nanostructure. Without extended optimization, a power conversion efficiency of 1.2% and a high V_{oc} of 0.731 V were achieved by using the PTcbpTT:PCBM (1:1 wt.%) blend annealed from the liquid-crystalline state as the active layer, which is superior to that of the copolymer cells as-prepared (0.5%) under the same experimental conditions. It is observed that the thermal annealing in liquid crystalline of the PTcbpTT:PCBM film, leads to an overall enhanced photovoltaic performance, including J_{sc}, FF, and PCE. A clear advantage of the photocrosslinking strategy is that crosslinking can be decoupled from thermal annealing, a valuable feature for BHJ solar cells that require some annealing to achieve optimum nanomorphology before crosslinking, and freeze this optimum morphology and preserve long term performance.

Acknowledgments

This work was supported by the National Natural Science Foundation of China (51073076, 51003045, 51172103 and 50902067).

Appendix A. Supplementary material

Supplementary data associated with this article can be found, in the online version, at doi:10.1016/j.orgel.2011.10.012.

References

[1] C.J. Brabec, N.S. Sariciftci, J.C. Hummelen, Adv. Funct. Mater. 11 (2001) 15–26.
[2] B.C. Thompson, J.M.J. Fréchet, Angew. Chem. Int. Ed. 47 (2008) 58–77.
[3] S. Gunes, H. Neugebauer, N.S. Sariciftci, Chem. Rev. 107 (2007) 1324–1338.
[4] M. Helgesen, R. Søndergaard, F.C. Krebs, J. Mater. Chem. 20 (2010) 36–60.
[5] G. Yu, J. Gao, J.C. Hummelen, F. Wudl, A.J. Heeger, Science 270 (1995) 1789–1791.
[6] H. Xin, F.S. Kim, S.A. Jenekhe, J. Am. Chem. Soc. 130 (2008) 5424–5425.
[7] M.M. Wienk, M. Turbiez, J. Gilot, R.A.J. Janssen, Adv. Mater. 20 (2008) 2556–2560.
[8] J.K. Lee, W.L. Ma, C.J. Brabec, J. Yuen, J.S. Moon, J.Y. Kim, K. Lee, G.C. Bazan, A.J. Heeger, J. Am. Chem. Soc. 130 (2008) 3619–3623.
[9] M. Reyes-Reyes, K. Kim, D.L. Carroll, Appl. Phys. Lett. 87 (2005) 083506.
[10] J.Y. Kim, K. Lee, N.E. Coates, D. Moses, T.Q. Nguyen, M. Dante, A.J. Heeger, Science 317 (2007) 222–225.
[11] W.L. Ma, C.Y. Yang, X. Gong, K. Lee, A.J. Heeger, Adv. Funct. Mater. 15 (2005) 1617–1622.
[12] B.A. Gregg, MRS Bull. 30 (2005) 20–22.
[13] I.W. Hwang, Q.H. Zhu, C. Soci, B.Q. Chen, A.K.Y. Jen, D. Moses, A.J. Heeger, Adv. Funct. Mater. 17 (2007) 563–568.
[14] H. Ohkita, S. Cook, Y. Astuti, W. Duffy, S. Tierney, W. Zang, M. Heeney, I. McCulloch, J. Nelson, D.C.C. Bradley, J.R. Durrant, J. Am. Chem. Soc. 130 (2008) 3030–3042.
[15] K. Yao, Y.W. Chen, L. Chen, D. Zha, F. Li, J.N. Pei, Z.Y. Liu, W.J. Tian, J. Phys, Chem. C 114 (2010) 18001–18011.
[16] C.J. Brabec, M. Heeney, I. McCulloch, Nelson, J. Chem. Soc. Rev. 40 (2011) 1185–1199.
[17] S. Gunes, H. Neugebauer, N.S. Sariciftci, Chem. Rev. 107 (2007) 1324–1328.
[18] B.J. Kim, Y. Miyamoto, B. Ma, J.M.J. Fréchet, Adv. Funct. Mater. 19 (2009) 2273–2281.
[19] M. Drees, H. Hoppe, C. Winder, H. Neugebauer, N.S. Sariciftci, W. Schwinger, F. Schaffler, C. Topf, M.C. Scharber, Z.G. Zhu, R. Gaudiana, J. Mater. Chem. 15 (2005) 5158–5163.
[20] Z. Zhu, S. Hadjikyriacou, D. Waller, R. Gaudiana, J. Macromol, Sci., Part A: Pure Appl. Chem. 41 (2004) 1467–1487.
[21] K. Ueyama, Macromolecules 40 (2007) 2277–2288.
[22] F.H.G. Bergmann, H. Finkelmann, Macromol. Rapid Commun. 18 (1997) 353–360.
[23] C.J. Dubois, L.P. Barny, M. Mauzac, C. Noel, Acta Polym. 48 (1997) 47–87.
[24] D. Zhang, Y. Liu, X. Wan, Q. Zhou, Macromolecules 32 (1999) 4494–4496.
[25] H. Goto, S. Nimori, K. Akagi, Synth. Met. 155 (2005) 576–587.
[26] H. Goto, X. Dai, T. Ueoka, K. Akagi, Macromolecules 37 (2004) 4783–4793.
[27] P. Ibison, S.J.P. Foot, W.J. Brown, Synth. Met. 76 (1996) 297–300.
[28] K. Yao, Y.W. Chen, L. Chen, F. Li, X.E. Li, X.Y. Ren, H.M. Wang, T.X. Liu, Macromolecules 44 (2011) 2698–2706.
[29] D. Zhou, Y.W. Chen, L. Chen, W.H. Zhou, X.H. He, Macromolecules 42 (2009) 1454–1461.
[30] G. Li, V. Shrotriya, J. Huang, Y. Yao, T. Mariarty, K. Emery, Y. Yang, Nat. Mater. 4 (2005) 864–868.
[31] L.M. Chen, Z.R. Hong, G. Li, Y. Yang, Adv. Mater. 21 (2009) 1434–1449.
[32] X. Yang, J. Loos, S.C. Veenstra, W.J.H. Verhees, M.M. Wienk, J.M. Kroons, M.A.J. Michels, R.A.J. Janssen, Nano Lett. 5 (2005) 579–583.
[33] M. Manceau, M. Helgesen, F.C. Krebs, Polym. Degradation Stability 95 (2010) 2666–2669.
[34] S. Bertho, G. Janssen, T.J. Cleij, B. Conings, W. Moons, A. Gadisa, J. D'Haen, E. Goovaerts, L. Lutsen, J. Manca, D. Vanderzande, Solar Energy Mater. Solar Cells 92 (2008) 753–760.
[35] S. Bertho, I. Haeldermans, A. Swinnen, W. Moons, T. Martens, L. Lutsen, D. Vanderzande, J. Manca, A. Senes, A. Bonfiglio, Solar Energy Mater. Solar Cells 91 (2007) 385–389.
[36] C. Müller, J. Bergqvist, K. Vandewal, K. Tvingstedt, A.S. Anselmo, R. Magnusson, M.I. Alonso, E. Moons, H. Arwin, M. Campoy-Quiles, O. Inganäs, J. Mater. Chem. 21 (2011) 10676–10684.
[37] G. Griffini, J.D. Douglas, C. Piliego, T.W. Holcombe, S. Turri, J.M.J. Fréchet, J.L. Mynar, Adv. Mater. 23 (2011) 1660–1664.
[38] K.S. Lee, K.Y. Yeon, K.H. Jung, S.K. Kim, J. Phys. Chem. A 112 (2008) 9312–9317.
[39] Y.R. Lee, C.C. Chen, S.M. Lin, J. Chem. Phys. 118 (2003) 10494.
[40] Y. Tang, L. Ji, R.S. Zhu, Z.R. Wei, B. Zhang, J. Phys. Chem. A 109 (2005) 11123–11126.
[41] Y. Zhao, Z. Xie, Y. Qu, Y. Geng, L. Wang, Appl. Phys. Lett. 90 (2007) 043504.
[42] Q. Sun, K. Park, L. Dai, J. Phys. Chem. C 113 (2009) 7892–7897.